Atmos. Chem. Phys., 24, 13361–13370, 2024
https://doi.org/10.5194/acp-24-13361-2024

Atmospheric Chemistry and Physics
Open Access
EGU

Multi-model effective radiative forcing of the 2020 sulfur cap for shipping

Ragnhild Bieltvedt Skeie, Rachael Byrom, Øivind Hodnebrog, Caroline Jouan, and Gunnar Myhre

CICERO Center for International Climate Research, Oslo, Norway

Correspondence: Ragnhild Bieltvedt Skeie (r.b.skeie@cicero.oslo.no)

Received: 13 May 2024 – Discussion started: 24 May 2024
Revised: 6 September 2024 – Accepted: 28 September 2024 – Published: 4 December 2024

Abstract. New regulations of sulfur emissions from shipping were introduced in 2020, reducing emissions of SO_2 from international shipping by $\sim 80\,\%$. As SO_2 is an aerosol precursor, this drop in emissions over the ocean will weaken the total aerosol effective radiative forcing (ERF) that has historically masked an uncertain fraction of the warming due to the increased concentration of greenhouse gases in the atmosphere. Here, we use four global climate models and a chemical transport model to calculate the ERF resulting from an 80 % reduction in SO_2 emissions from international shipping relative to 2019 emission estimates. The individual model means range from 0.06 to 0.09 $W\,m^{-2}$, corresponding to the ERF resulting from the increase in CO_2 concentration over the last 2 to 3 years. The full uncertainty in the ERF due to the new regulation is not quantified but will very likely be high considering the contribution of uncertainties in shipping SO_2 emissions, the sulfur cycle, the modelling of cloud adjustments and the impact of interannual variability on the method for calculating radiative forcing.

1 Introduction

On 1 January 2020, the International Maritime Organization (IMO) regulation on the limitation of sulfur in shipping fuel (IMO, 2018) entered into force. This rule, hereafter named IMO2020, reduces the allowed sulfur content of marine fuels used outside of emission control areas from 3.5 % to 0.5 %. To fulfil the regulation, ships must either use low-sulfur fuel or install scrubbers that remove SO_2 from the exhaust, and this new regulation will lead to a 77 % reduction in total SO_2 emissions from shipping (Corbett et al., 2016).

Emission of sulfur dioxide (SO_2) from shipping impacts air quality, is harmful for human health, has negative consequences for ecosystems and affects climate (Eyring et al., 2010). Through chemical reactions in the atmosphere, the emitted SO_2 is transformed into sulfate particles. Sulfate particles can alter the energy balance at the top of the atmosphere (TOA), either directly by reflecting solar radiation or indirectly by modifying cloud properties, which are quantified by the effective radiative forcing (ERF) of aerosol–radiation interaction (ERFari) and aerosol–cloud interaction (ERFaci). The ERF metric includes the radiative effects of atmospheric adjustments to the initial forcing that are not mediated by surface temperature change. Such so-called "rapid adjustments" include changes in stratospheric temperature, tropospheric temperature, water vapour, surface albedo and clouds (Smith et al., 2018; Boucher et al., 2013; Sherwood et al., 2015). Changes in cloud liquid water path and cloud cover comprise the main cloud adjustments and are associated with large uncertainties (Bellouin et al., 2020). When all tropospheric adjustments are excluded (i.e. only stratospheric temperatures are adjusted), the forcing is termed radiative forcing (RF). This can be divided into RF of aerosol–radiation interaction (RFari), which represents the interaction of aerosol particles themselves with the radiation field, and RF of aerosol–cloud interaction (RFaci), which accounts for how aerosol particles change the reflectivity of clouds by altering the cloud droplet number concentration. The adjustments following aerosol–radiation interaction for a sulfate perturbation are negligible as sulfate aerosols are non-absorbing (Stjern et al., 2023).

SO_2 is the dominant contributor to the aerosol ERF and was assessed to be $-0.94 \pm 0.69\,W\,m^{-2}$ (90 % confidence

interval) in 2019 relative to 1750, with a dominant contribution from ERFaci (Szopa et al., 2021). The total aerosol ERF is assessed to be $-1.3 \pm 0.7\,\mathrm{W\,m^{-2}}$ (90 % confidence interval) over the industrial era (1750–2014) (Forster et al., 2021).

The total sulfur emissions from international shipping in 2019 amounted to $10.9\,\mathrm{Tg\,SO_2\,yr^{-1}}$, which is 13 % of the total anthropogenic emissions of SO_2 (O'Rourke et al., 2021). The SO_2 emissions from international shipping increased steadily from the 1980s to a maximum of $14\,\mathrm{Tg\,SO_2\,yr^{-1}}$ in 2008 (Fig. S1 in the Supplement). Over the same period, the total anthropogenic SO_2 emissions decreased, and the relative contribution of international shipping emissions increased. Approximating the reduction in SO_2 emissions from the shipping sector to be 80 % in 2020, the emissions would have dropped by $8.7\,\mathrm{Tg\,yr^{-1}}$, corresponding to a 10 % reduction in the total anthropogenic SO_2 emissions in 2019.

Eyring et al. (2010) summarised previous studies of the radiative forcing of the shipping sector and came up with a best estimate of the SO_2 radiative forcing direct effect (aerosol–radiation interaction) of $-0.031\,\mathrm{W\,m^{-2}}$ in 2005; on the other hand, the estimates of the aerosol radiative forcing indirect effect (aerosol–cloud interaction) ranged from $-0.066\,\mathrm{W\,m^{-2}}$ (Fuglestvedt et al., 2008) up to $-0.6\,\mathrm{W\,m^{-2}}$ (Lauer et al., 2007). However, the estimate of Lauer et al. (2007) included other aerosols in addition to sulfate and had a large sensitivity to the assumption of geographical emission distribution. Subsequently, their estimate was as large as 39 % of the total indirect aerosol radiative forcing (Eyring et al., 2010).

Several studies have looked at the radiative effects of sulfur emission reductions in international shipping that correspond to IMO2020. Note that this regulation was discussed and adopted by the IMO several years prior to its implementation, allowing for the modelled projection of its associated climate impact. Partanen et al. (2013) found a large shipping radiative forcing of $0.33\,\mathrm{W\,m^{-2}}$ following an 89 % reduction in 2020 SO_2 emissions relative to 2010 using the ECHAM-HAMMOZ model. Jin et al. (2018) calculated a $0.23\,\mathrm{W\,m^{-2}}$ forcing following a reduction in the SO_2 fuel content of shipping from 3.5 % to 0.5 % using CESM1.2.2, and Sofiev et al. (2018) reported a forcing of $0.071\,\mathrm{W\,m^{-2}}$ using the SILAM chemical transport model that accounted for the direct aerosol effect and the effect of lowering the cloud albedo. More recently, Bilsback et al. (2020) found a smaller ERF of just $0.027\,\mathrm{W\,m^{-2}}$ for an 85 % reduction in SO_2 emissions from the shipping sector using GEOS-Chem-TOMAS. Gettelman et al. (2024) found an ERF of $0.12\,\mathrm{W\,m^{-2}}$ by applying an 80 % reduction in shipping emissions from a 2015 baseline using three Earth system models with nudged meteorology.

The effect of ship emission regulations can also be observed from space via ship tracks. These provide a visualisation of aerosol–cloud interactions along the route of travel due to the enhanced concentration of sulfate particles which act as cloud condensation nuclei and cause an increase in the number of droplets within a cloud. A higher number of droplets makes the cloud brighter and identifiable in satellite imagery. Yuan et al. (2022) and Watson-Parris et al. (2022) both reported a reduction in the presence of ship tracks after IMO2020 entered into force. However, cloud properties where ship tracks are not visible are also found to be impacted by ship emissions (Manshausen et al., 2022); therefore, studying ship tracks alone to estimate ERFaci will introduce selection biases (Glassmeier et al., 2021).

In this study, we use four different global climate models and one chemical transport model (CTM) to diagnose the ERF of an 80 % reduction in shipping SO_2 emissions from the same baseline, corresponding to the worldwide emission reductions associated with IMO regulations that came into play in 2020.

Table 1. Models included in the study, number of ensembles and length of the simulation. Note that OsloCTM3 is a CTM run with fixed meteorology, and 1 year is sufficient for calculations of radiative forcing.

Model	No. of ensemble members	Simulation length
CESM2	2	100 years
ModelE_MATRIX	2	50 years
ModelE_OMA	2	50 years
NorESM2	2	200 years
OsloCTM3	1	1 year

2 Method

We use four global climate models (Table 1) to perform two types of atmosphere-only simulations: one baseline integration with 2019 anthropogenic aerosol (and precursor) emissions (CNTR) and one perturbed integration where SO_2 and SO_4 emissions from shipping are reduced by 80 % (20perc-SHP). The resulting forcing is calculated as the difference in top-of-atmosphere net radiative flux between the two simulations. As recommended by the Radiative Forcing Model Intercomparison Project (RFMIP, Forster et al., 2016; Smith et al., 2020), we calculate ERF using fixed sea surface temperatures and sea ice climatology. For each global climate model, we run two ensemble members which differ in terms of the climatologies of sea surface temperatures and sea ice concentrations that are used in the simulations (ensemble member 1 uses the 2000 climatology, and ensemble member 2 uses the 2010 climatology).

Each model is run for the simulation length specified in Table 1. Given that the potential impact of IMO2020 on radiative fluxes could be relatively small (e.g. Jin et al., 2018; Sofiev et al., 2018; Bilsback et al., 2020), these lengths needed to be sufficiently long to reduce the signal-to-noise ratio in the ERF calculation (Forster et

al., 2016). ModelE_MATRIX and ModelE_OMA do not include cloud adjustments; therefore, the forcing diagnosed is RF. NorESM2 and CESM2 include cloud adjustments, and ERF is diagnosed. We further use a CTM (Table 1) and an offline radiative transfer model to analyse the RF in more detail by calculating the RFari and RFaci associated with the 2020 shipping emission cap. Results from a CTM are not influenced by noise, and, therefore, a simulation length of 1 year is sufficient. Although cloud adjustments are not included in all models, we present the results collectively as ERF.

In all simulations, we use 2019 anthropogenic aerosol (and precursor) emissions from the Community Emissions Data System (CEDS) (v_2021_02_05, O'Rourke et al., 2021), which builds upon the CEDS inventory described in McDuffie et al. (2020), hereafter named CEDS_v2021. In the following, a short description of each model and their individual configurations and setups is provided.

2.1 CESM2

The Community Earth System Model 2 (CESM2) has been used with the Community Atmosphere Model Version 6 (CAM6) atmospheric module (Danabasoglu et al., 2020). Greenhouse gas (GHG) concentrations are representative of the year 2000's climatology, while anthropogenic aerosol (precursor) emissions are from the year 2019 from the CEDS_v2021. The model has been set up with a horizontal resolution of $1.9° \times 2.5°$ and 32 vertical layers. Aerosol physics are treated according to the Modal Aerosol Module version 4 (Liu et al., 2016), cloud droplet activation parameterisation is based on Abdul-Razzak and Ghan (2000), and aerosol–cloud interactions are included.

2.2 NASA GISS ModelE

Two versions of the Goddard Institute of Space Sciences Earth System Model (GISS ModelE version 2.1.2) developed by NASA (National Aeronautics and Space Administration) (Kelley et al., 2020) are used. The two versions differ in terms of the aerosol scheme used (Bauer et al., 2020), i.e. the two-moment MATRIX (Multiconfiguration Aerosol TRacker of mIXing state) scheme in which all aerosols are internally mixed, hereafter named ModelE_MATRIX, or the One-Moment Aerosol (OMA) scheme in which aerosols are assumed to remain externally mixed, hereafter named ModelE_OMA. As ModelE_OMA and ModelE_MATRIX have different aerosol physics, we treat these as two separate models in this study. In MATRIX, the cloud droplet activation parameterisation is based on Abdul-Razzak and Ghan (2000), while in OMA, the aerosol conversion into cloud condensation nuclei is empirical, following the method outlined by Menon and Rotstayn (2006). MATRIX and OMA only include the effect of aerosol on the cloud droplet concentrations (Bauer et al., 2020) and, hence, do not include changes in the cloud liquid water path.

Greenhouse gas concentrations are representative of the year 1994's climatology, while anthropogenic aerosol and aerosol precursor emissions are the CEDS_v2021 emissions for the year 2019. Both ModelE_OMA and ModelE_MATRIX have a horizontal resolution of 2.0° in latitude by 2.5° in longitude and 40 vertical layers, extending from the surface to 0.1 hPa.

2.3 NorESM2

The Norwegian Earth System Model version 2 (NorESM2) is developed by the Norwegian Center for Climate Services (Seland et al., 2020). Here, we use the "LM" version which has a "low" horizontal resolution ($1.9° \times 2.5°$) in the atmosphere. The atmospheric component (CAM6-Nor) is built on CESM2.1 CAM6 but uses a different module (OsloAero6, Kirkevåg et al., 2018) for aerosol chemistry and physics, including aerosol–cloud radiation interactions. As in both CESM2 and MATRIX, the cloud droplet activation parameterisation in CAM6-Nor is based on Abdul-Razzak and Ghan (2000) (see also Kirkevåg et al., 2013). CAM6-Nor has 32 vertical layers with a model top around 2.26 hPa. GHG concentrations represent climatology from the year 2000, with aerosol and aerosol precursor emissions representing the year 2019 from CEDS_v2021.

2.4 OsloCTM3

OsloCTM3 (Lund et al., 2018; Søvde et al., 2012) is an offline global three-dimensional chemical transport model driven by 3 hourly meteorological forecast data from the Open Integrated Forecast System (Open IFS, cycle 38, revision 1) at the European Centre for Medium-Range Weather Forecasts (ECMWF). In this study, the model is driven by 2010 meteorology, with the year 2009 used as spin-up, and CEDS_v2021 anthropogenic emissions. The horizontal resolution is $\sim 2.25° \times 2.25°$, and, in the vertical, the model is made up of 60 layers ranging from the surface up to 0.1 hPa. OsloCTM3 consists of a tropospheric and stratospheric chemistry scheme (Søvde et al., 2012), as well as aerosol modules for sulfate, nitrate, black carbon, primary organic carbon, secondary organic aerosols, mineral dust and sea salt (Lund et al., 2018). The aerosol radiative forcing is calculated offline (Myhre et al., 2017) from the 3 hourly output from OsloCTM3. For aerosol–cloud interaction, only the change in effective radius is simulated, so no rapid adjustments to microphysical properties such as cloud fraction or liquid water content are considered. Thus, for the OsloCTM3, we report aerosol RF and not aerosol ERF.

3 Results

For each model and each ensemble member, the ERF due to the 80 % reduction in SO_2 emissions from shipping is calculated and presented in Fig. 1. The mean values for each

individual ensemble range from 0.035 to 0.11 W m^{-2}. The mean ERF for the individual models ranges from 0.057 to 0.089 W m^{-2} (the orange bar in Fig. 1).

As the signal is small, the simulation length needs to be long to assess the ERF in the climate models (Table 1). Also shown in Fig. 1 are the 66 %, 90 % and 95 % confidence intervals (CIs) calculated from the net radiation at the top of the atmosphere over the entire simulation length. For two of the ensemble members, the lower ends of the 95 % CIs for the ERFs are less than 0.0. There is also considerable spread between the individual ensemble members. For two of the models, ModelE_OMA and NorESM2, the mean value for one of the ensemble members is outside of the 66 % CI of the other ensemble member.

For OsloCTM3, ModelE_MATRIX and ModelE_OMA, the cloud adjustments to the shipping emission perturbations are not included (see Sect. 2), and what we report for these models is the RF. Their mean RF ranges from 0.066 to 0.086 W m^{-2}, similarly to the range for NorESM2 and CESM2 of 0.057 to 0.089 W m^{-2}, which includes the cloud adjustments. This might indicate that cloud adjustments play a limited role in CESM2 and NorESM2. For OsloCTM3, we can split the RF into RFari and RFaci. The geographical distributions of these results are shown in Fig. 2, with the strongest RFaci in the northeastern Atlantic and northeastern Pacific. The global-mean RFari is 0.024 W m^{-2}, and the global-mean RFaci is 0.045 W m^{-2}, contributing 35 % and 65 %, respectively, to the total RF of the 80 % SO_2 emission reduction in OsloCTM3.

The geographical distributions of the ERF for the individual ensemble members are noisy (Fig. S2) due to internal variability, which is amplified by the weather patterns influencing the source of natural forcers, such as dust and sea salt aerosols. For the model means and the multi-model mean (Fig. 3), positive ERFs in the North Atlantic, northeastern Pacific and northwestern Pacific are seen. These are areas where the models agree on the sign of the ERF, as indicated with hatching in Fig. 3.

The strongest ERF is in the North Atlantic, with values of up to 0.78 W m^{-2} in the multi-model mean. Note that the 80 % reduction in shipping emissions was applied globally, including in areas with already strict emission controls; hence, emission reductions in the global ocean may have been even larger than what is used in the simulations, and the maximum ERF values may have been underestimated.

The 80 % reduction in SO_2 emissions from the shipping sector is driving these forcing responses. The SO_2 emissions chemically react in the atmosphere and are converted to sulfate particles that alter the radiation field directly or indirectly via clouds in the atmosphere before the particles are eventually removed through scavenging. Table 2 summarises the SO_4 burden change due to the emission reduction in the shipping sector from the individual ensemble members in each model. The SO_4 burden change ranges from −0.018 to −0.070 Tg (−1.5 % to −2.7 %) for the same emission perturbation of 8.7 Tg SO_2 yr^{-1}, indicating that differences in the representation of the sulfur cycle contribute to the model spread in the forcing.

As shown in Fig. S1, the total anthropogenic emissions of SO_2 have decreased over the last 3 decades but with large regional differences (O'Rourke et al., 2021). The simulated 1-year change in the near-surface mass mixing ratio of sulfate from OsloCTM3 for an 80 % reduction in ship emissions has a different geographical distribution than historical sulfur changes, as simulated by OsloCTM3 (Skeie et al., 2023), and also shows a large reduction per year (Fig. S3). Considering longer time periods, the historical change in sulfur overwhelms this 1-year drop in shipping emissions in 2020, including over the oceanic regions with the strongest shipping reductions (Fig. S3).

4 Discussion and conclusion

In this multi-model study, the mean ERFs for an 80 % reduction in SO_2 emissions from shipping range from 0.057 to 0.089 W m^{-2} in individual models, with a multi-model mean of 0.073 W m^{-2}. Previous estimates of the climate forcing of the IMO shipping regulations in 2020 using single models and different assumptions regarding the emission reductions show a wider range of 0.03 to 0.33 W m^{-2} (Sofiev et al., 2018; Bilsback et al., 2020; Jin et al., 2018; Partanen et al., 2013). The uncertainty calculated based on the interannual variability in the individual ensemble members is larger than the spread in the model mean estimates (Fig. 1). This highlights the importance of simulations with sufficient length for the ERF calculations. In addition to uncertainties related to interannual variability in the simulations, there are additional uncertainties as discussed below.

To calculate the ERF of the 2020 shipping emission regulation in this study, the shipping emissions are scaled by a single factor so that the total emissions from the shipping sector are reduced by 80 %. This is a simplified test and does not consider the fact that emissions in specific areas already had strict emission regulations prior to 2020. However, there is substantial uncertainty with regard to total sulfur emissions from the shipping sector; for example, Eyring et al. (2010) estimated a large uncertainty range of 3 to 10 Tg S yr^{-1} for the year 2000. Uncertainty in baseline emissions hence causes uncertainty in emission reductions due to the new regulation. Recently, a new CEDS inventory (Hoesly and Smith, 2024) became available, extending emissions until 2022 (Fig. S1) with a 71 % reduction in sulfur emissions from international shipping in 2020 relative to 2019, which is lower than the emission perturbation used in our simulations. IMO2020 can also be complied with alternate methods, either by switching to low-sulfur fuel or by wet scrubbing of the exhaust. Each method results in different physical properties of the exhaust particles and, hence, produces different impacts on clouds (Santos et al., 2024).

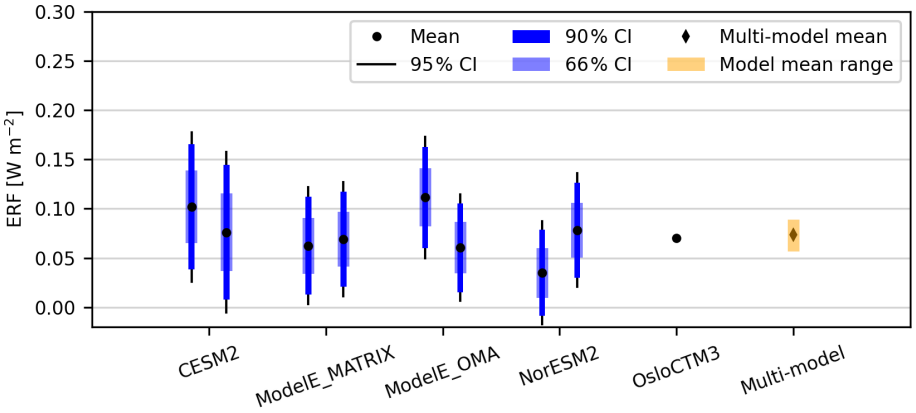

Figure 1. Effective radiative forcing for an 80 % reduction in shipping emissions as calculated in the models. Each ensemble member is plotted separately, and the mean ERF value (black dot), the 66 % confidence interval (thick coloured bar), the 90 % confidence interval (thin coloured bar) and the 95 % confidence interval (vertical solid line) based on the interannual variations are shown. The lengths of the ensemble members for the individual models are given in Table 1. OsloCTM3, ModelE_MATRIX and ModelE_OMA report RF since cloud adjustments are not included. For OsloCTM3, the calculated RF value is shown as a black dot. The multi-model mean is indicated by a black diamond. The range of the model means (taken as the mean of the ensemble means) is shown as an orange bar.

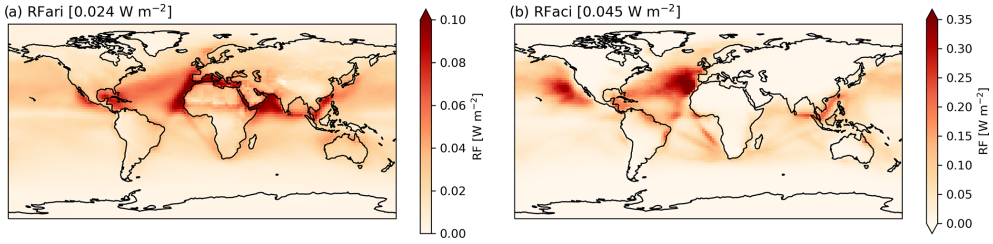

Figure 2. RFari **(a)** and RFaci **(b)** from OsloCTM3 for an 80 % sulfur emission reduction in shipping. Note the different colour scale in the two figures.

Such effects are not included in global chemistry models and cannot be derived from emission estimates.

In marine areas, dimethyl sulfide (DMS) is an important sulfur component, and the models included in this study span a large range of natural DMS emissions from 27 to 60 Tg DMS yr^{-1} (Table 2). Jin et al. (2018) highlighted the significance of the natural DMS concentration for aerosol–cloud interactions due to shipping emissions. When DMS emissions in their simulations were reduced, the cloud radiative effect of the shipping emission reduction increased. Measurements of DMS from the airborne NASA Atmospheric Tomography (ATom) mission indicate that the DMS emissions in global models may be overestimated (Bian et al., 2024). A set of simulations with DMS emissions reduced to 30 Tg DMS yr^{-1} in the OsloCTM3 result in a similar decrease in sulfate burden (in absolute values) for the 80 % emission reduction from the shipping sector, while the RFaci showed an increase of 23 %. The OsloCTM3 is the model with the largest DMS emissions, but it is also the model with the largest absolute change in sulfate burden among the models included in this study (Table 2). Therefore, a better representation of the sulfur cycle in marine areas is needed to further our understanding of the impact of SO_2 emissions on climate.

The ERFaci due to SO_2 emissions from shipping includes the formation of ship tracks. The global models are unable to explicitly represent these small-scale processes. Watson-Parris et al. (2022) used machine learning to detect all ship tracks in satellite data. They found only a 25 % reduction in ship track frequency following the implementation of IMO2020. Shipping emissions also interact with clouds and change cloud properties even if ship tracks are not visible in satellite images (Glassmeier et al., 2021; Manshausen et al., 2022). Diamond (2023) used a statistical technique to look at the large-scale cloud properties in the southeastern Atlantic from satellite images and found a reduction in the magnitude of the cloud droplet effective radius and cloud brightening. He estimated the forcing within the shipping corridor from the IMO2020 regulations, which implied a global instantaneous radiative forcing due to aerosol–cloud interactions of 0.1 W m^{-2}, similar in magnitude to the multi-model mean ERF calculated in this study.

The models included in this study have a variable degree of microphysical cloud adjustments. OsloCTM3,

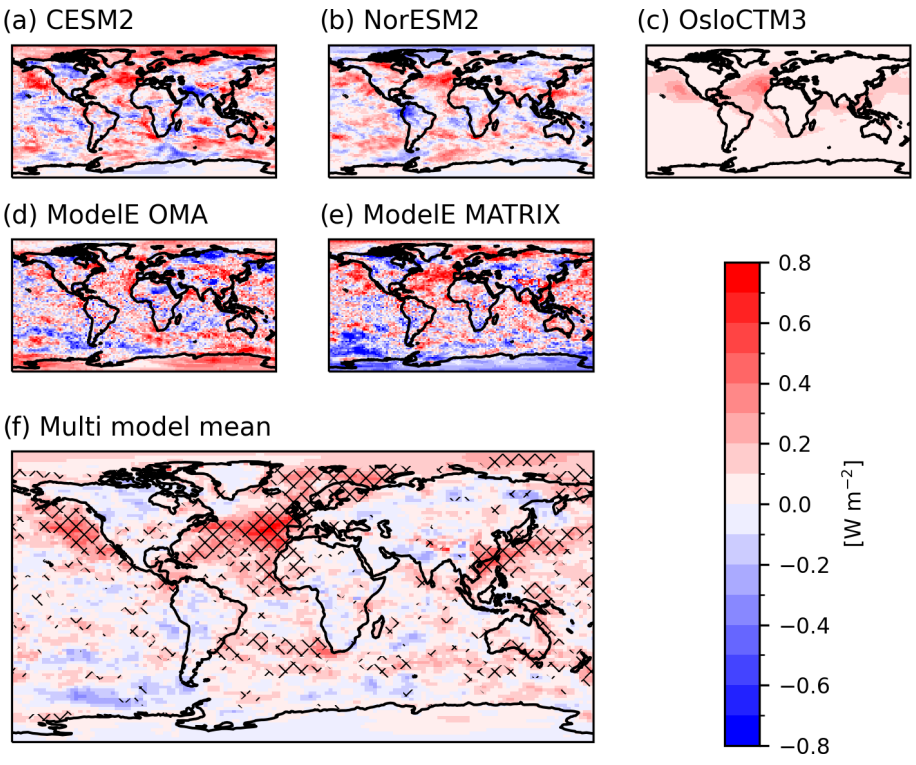

Figure 3. The model mean **(a–e)** and **(f)** the multi-model mean of the ERF for 80 % reduction in shipping emissions. The multi-model mean is calculated from the individual model means **(a–e)** re-gridded to a similar grid before calculating the mean. The hatching indicates areas where at least four out of five models have the same sign of ERF.

Table 2. Absolute (in Tg SO_4) and relative change (in %) in sulfate burden between 20percSHP and CNTR and DMS emissions in CNTR and 20percSHP (in Tg DMS yr^{-1}). The results for the ensemble members are shown separately, and the standard error is based on the interannual variability given.

Model	No. of ensemble member	SO_4 burden change (20percSHP − CNTR) (Tg SO_4)	Relative change in SO_4 burden (20percSHP − CNTR) (%)	DMS emissions in CNTR (Tg DMS yr^{-1})	DMS emissions in 20percSHP (Tg DMS yr^{-1})
CESM2	1	-0.0325 ± 0.002	-1.9 ± 0.1	26.9*	26.9
	2	-0.0283 ± 0.002	-1.6 ± 0.1	26.9	26.9
ModelE_MATRIX	1	-0.0465 ± 0.002	-2.2 ± 0.1	54.6 ± 0.1	54.6 ± 0.1
	2	-0.0571 ± 0.002	-2.7 ± 0.1	54.8 ± 0.1	54.8 ± 0.1
ModelE_OMA	1	-0.0247 ± 0.002	-1.8 ± 0.1	54.4 ± 0.1	54.5 ± 0.1
	2	-0.0281 ± 0.002	-2.1 ± 0.1	54.7 ± 0.1	54.8 ± 0.1
NorESM2	1	-0.0176 ± 0.001	-1.5 ± 0.1	43.8 ± 0.03	43.8 ± 0.03
	2	-0.0195 ± 0.001	-1.6 ± 0.1	43.7 ± 0.03	43.8 ± 0.03
OsloCTM3	1	−0.0701	−2.7	60.0	60.0

* DMS emissions are prescribed in CESM2.

ModelE_GISS and ModelE_MATRIX do not include changes in liquid water path and cloud cover, and, hence, RF is reported. The models reporting RF and the models reporting ERF show a similar spread, which may indicate a limited role of cloud adjustments in the two other models. Note also that there are similarities in the cloud droplet activation parameterisation in the models (see Sect. 2) that may reduce the model spread. Using satellite retrievals, reanalysis winds, ship positions and modelled shipping emissions, Manshausen et al. (2023) showed that the increase in liq-

uid water content is constant over a wide range of emission perturbations which are caused by the compensating effects of increases and decreases in liquid water path in different regimes. They also found that liquid water path anomalies are largely unchanged before and after 2020, and so the liquid water path adjustments were weak due to the ship emission regulation. This indicates that chemistry models without detailed representation of the liquid water path adjustments do not largely underestimate the ERF of the shipping emission cap. A remaining issue that Manshausen et al. (2023) highlighted is how the ship emission regulations have impacted the cloud fraction in observation-based studies (Chen et al., 2022, 2024). The recent study by Yuan et al. (2024) found the cloud fraction adjustments to contribute by 60 % to their forcing estimate of 0.2 $\mathrm{W\,m^{-2}}$ (for the global ocean) when combining satellite data and global modelling, while liquid water path adjustments were negligible at the global scale.

Shipping emission regulation has been suggested as a possible reason for the increase in the Earth's energy imbalance as measured by CERES (Clouds and Earth's Radiant Energy System) over the last years and as a contributor to the acceleration of global warming (Hansen et al., 2023). The multi-model mean ERF due to IMO2020 is estimated to be 0.073 $\mathrm{W\,m^{-2}}$, with individual model means ranging from 0.057 to 0.089 $\mathrm{W\,m^{-2}}$. To put the results in context, an ERF of $\sim$0.1 $\mathrm{W\,m^{-2}}$ for the IMO2020 regulation is comparable to the increase in CO_2 ERF of 0.1 $\mathrm{W\,m^{-2}}$ from 2019 to 2022 (Forster et al., 2023). However, it is important to keep in mind that the ERF for the IMO2020 shipping cap calculated in this study has large uncertainties (as for aerosol ERF in general) related specifically to cloud adjustments, emission uncertainties and uncertainties in the sulfur cycle.

Code availability. The code to reproduce the figures in this paper can be found at https://zenodo.org/records/13710977 (Skeie, 2024).

Data availability. The data needed to reproduce the figures in the paper can be found at https://zenodo.org/records/13710977 (Skeie, 2024). The full dataset for the model results is available in the NIRD Research Data Archive: https://doi.org/10.11582/2024.00157 (Skeie et al., 2024). The CEDS emission inventories can be found at https://github.com/JGCRI/CEDS/ (last access: 5 September 2024) (https://doi.org/10.5281/zenodo.4741285, O'Rourke et al., 2021; https://doi.org/10.5281/zenodo.10904361, Hoesly and Smith, 2024).

Supplement. The supplement related to this article is available online at: https://doi.org/10.5194/acp-24-13361-2024-supplement.

Author contributions. RBS wrote the paper in collaboration with all the co-authors. RBS performed the OsloCTM3 simulations, ØH performed the CESM2 simulations, RB performed the NorESM2 simulations, and CJ performed the ModelE simulations. GM did the offline radiative transfer simulations.

Competing interests. At least one of the (co-)authors is a member of the editorial board of *Atmospheric Chemistry and Physics*. The peer-review process was guided by an independent editor, and the authors also have no other competing interests to declare.

Disclaimer. Publisher's note: Copernicus Publications remains neutral with regard to jurisdictional claims made in the text, published maps, institutional affiliations, or any other geographical representation in this paper. While Copernicus Publications makes every effort to include appropriate place names, the final responsibility lies with the authors.

Acknowledgements. We would like to thank Konstantinos Tsigaridis from NASA for his valuable assistance in setting up the NASA GISS ModelE. OsloCTM3, ModelE, CESM2 and NorESM2 simulations were performed using resources provided by Sigma2 – the national infrastructure for high-performance computing and data storage in Norway (project account no. NN9188K), and data were shared through their services (project NS9188K).

Financial support. This research has been supported by the Norges Forskningsråd (grant no. 314997) and the European Union's Horizon 2020 (grant no. 820829, CONSTRAIN).

Review statement. This paper was edited by Jason West and reviewed by two anonymous referees.

References

Abdul-Razzak, H. and Ghan, S. J.: A parameterization of aerosol activation: 2. Multiple aerosol types, J. Geophys. Res., 105, 6837–6844, https://doi.org/10.1029/1999JD901161, 2000.

Bauer, S. E., Tsigaridis, K., Faluvegi, G., Kelley, M., Lo, K. K., Miller, R. L., Nazarenko, L., Schmidt, G. A., and Wu, J.: Historical (1850–2014) Aerosol Evolution and Role on Climate Forcing Using the GISS ModelE2.1 Contribution to CMIP6, J. Adv. Model. Earth Sy., 12, e2019MS001978, https://doi.org/10.1029/2019MS001978, 2020.

Bellouin, N., Quaas, J., Gryspeerdt, E., Kinne, S., Stier, P., Watson-Parris, D., Boucher, O., Carslaw, K. S., Christensen, M., Daniau, A. L., Dufresne, J. L., Feingold, G., Fiedler, S., Forster, P., Gettelman, A., Haywood, J. M., Lohmann, U., Malavelle, F., Mauritsen, T., McCoy, D. T., Myhre, G., Mülmenstädt, J., Neubauer, D., Possner, A., Rugenstein, M., Sato, Y., Schulz, M., Schwartz, S. E., Sourdeval, O., Storelvmo, T., Toll, V., Winker, D., and Stevens, B.: Bounding Global Aerosol Radiative Forcing of Climate Change, Rev. Geophys., 58, e2019RG000660, https://doi.org/10.1029/2019RG000660, 2020.

Bian, H., Chin, M., Colarco, P. R., Apel, E. C., Blake, D. R., Froyd, K., Hornbrook, R. S., Jimenez, J., Jost, P. C., Lawler, M., Liu, M., Lund, M. T., Matsui, H., Nault, B. A., Penner, J. E., Rollins, A. W., Schill, G., Skeie, R. B., Wang, H., Xu, L., Zhang, K., and Zhu, J.: Observationally constrained analysis of sulfur cycle in the marine atmosphere with NASA ATom measurements and AeroCom model simulations, Atmos. Chem. Phys., 24, 1717–1741, https://doi.org/10.5194/acp-24-1717-2024, 2024.

Bilsback, K. R., Kerry, D., Croft, B., Ford, B., Jathar, S. H., Carter, E., Martin, R. V., and Pierce, J. R.: Beyond SO_x reductions from shipping: assessing the impact of NO_x and carbonaceous-particle controls on human health and climate, Environ. Res. Let., 15, 124046, https://doi.org/10.1088/1748-9326/abc718, 2020.

Boucher, O., Randall, D., Artaxo, P., Bretherton, C., Feingold, G., Forster, P., Kerminen, V.-M., Kondo, Y. Liao, H., Lohmann, U., Rasch, P., Satheesh, S. K., Sherwood, S., Stevens, B., and Zhang, X. Y.: Clouds and Aerosols, in: Climate Change 2013: The Physical Science Basis. Contribution of Working Group I to the Fifth Assessment Report of the Intergovernmental Panel on Climate Change, edited by: Stocker, T. F., Qin, D., Plattner, G.-K., Tignor, M., Allen, S. K., Boschung, J., Nauels, A., Xia, Y., Bex, V., and Midgley, P. M., Cambridge University Press, Cambridge, United Kingdom and New York, NY, USA, ISBN 978-1-107-05799-1, 2013.

Chen, Y., Haywood, J., Wang, Y., Malavelle, F., Jordan, G., Partridge, D., Fieldsend, J., De Leeuw, J., Schmidt, A., Cho, N., Oreopoulos, L., Platnick, S., Grosvenor, D., Field, P., and Lohmann, U.: Machine learning reveals climate forcing from aerosols is dominated by increased cloud cover, Nat. Geosci., 15, 609–614, https://doi.org/10.1038/s41561-022-00991-6, 2022.

Chen, Y., Haywood, J., Wang, Y., Malavelle, F., Jordan, G., Peace, A., Partridge, D. G., Cho, N., Oreopoulos, L., Grosvenor, D., Field, P., Allan, R. P., and Lohmann, U.: Substantial cooling effect from aerosol-induced increase in tropical marine cloud cover, Nat. Geosci., 17, 404–410, https://doi.org/10.1038/s41561-024-01427-z, 2024.

Corbett, J. J., Winebrake, J. J., Carr, E. W., Jalkanen, J.-P., Johansson, L., Prank, M., and Sofiev, M.: Health Impacts Associated with Delay of MARPOL Global Sulphur Standards, FMI, https://wwwcdn.imo.org/localresources/en/MediaCentre/HotTopics/Documents/Finland%20study%20on%20health%20benefits.pdf (last access: 6 September 2024), 2016.

Danabasoglu, G., Lamarque, J. F., Bacmeister, J., Bailey, D. A., DuVivier, A. K., Edwards, J., Emmons, L. K., Fasullo, J., Garcia, R., Gettelman, A., Hannay, C., Holland, M. M., Large, W. G., Lauritzen, P. H., Lawrence, D. M., Lenaerts, J. T. M., Lindsay, K., Lipscomb, W. H., Mills, M. J., Neale, R., Oleson, K. W., Otto-Bliesner, B., Phillips, A. S., Sacks, W., Tilmes, S., van Kampenhout, L., Vertenstein, M., Bertini, A., Dennis, J., Deser, C., Fischer, C., Fox-Kemper, B., Kay, J. E., Kinnison, D., Kushner, P. J., Larson, V. E., Long, M. C., Mickelson, S., Moore, J. K., Nienhouse, E., Polvani, L., Rasch, P. J., and Strand, W. G.: The Community Earth System Model Version 2 (CESM2), J. Adv. Model. Earth Sy., 12, e2019MS001916, https://doi.org/10.1029/2019MS001916, 2020.

Diamond, M. S.: Detection of large-scale cloud microphysical changes within a major shipping corridor after implementation of the International Maritime Organization 2020 fuel sulfur regulations, Atmos. Chem. Phys., 23, 8259–8269, https://doi.org/10.5194/acp-23-8259-2023, 2023.

Eyring, V., Isaksen, I. S. A., Berntsen, T., Collins, W. J., Corbett, J. J., Endresen, O., Grainger, R. G., Moldanova, J., Schlager, H., and Stevenson, D. S.: Transport impacts on atmosphere and climate: Shipping, Atmos. Environ., 44, 4735–4771, https://doi.org/10.1016/j.atmosenv.2009.04.059, 2010.

Forster, P., Storelvmo, T., Armour, K., Collins, W., Dufresne, J. L., Frame, D., Lunt, D. J., Mauritsen, T., Palmer, M. D., Watanabe, M., Wild, M., and Zhang, H.: The Earth's Energy Budget, Climate Feedbacks, and Climate Sensitivity, in: Climate Change 2021: The Physical Science Basis. Contribution of Working Group I to the Sixth Assessment Report of the Intergovernmental Panel on Climate Change, edited by: Masson-Delmotte, V., Zhai, P., Pirani, A., Connors, S. L., Péan, C., Berger, S., Caud, N., Chen, Y., Goldfarb, L., Gomis, M. I., Huang, M., Leitzell, K., Lonnoy, E., Matthews, J. B. R., Maycock, T. K., Waterfield, T., Yelekçi, O., Yu, R., and Zhou, B., Cambridge University Press, Cambridge, United Kingdom and New York, NY, USA, https://doi.org/10.1017/9781009157896.009, 2021.

Forster, P. M., Richardson, T., Maycock, A. C., Smith, C. J., Samset, B. H., Myhre, G., Andrews, T., Pincus, R., and Schulz, M.: Recommendations for diagnosing effective radiative forcing from climate models for CMIP6, J. Geophys. Res., 121, 12460–12475, https://doi.org/10.1002/2016JD025320, 2016.

Forster, P. M., Smith, C. J., Walsh, T., Lamb, W. F., Lamboll, R., Hauser, M., Ribes, A., Rosen, D., Gillett, N., Palmer, M. D., Rogelj, J., von Schuckmann, K., Seneviratne, S. I., Trewin, B., Zhang, X., Allen, M., Andrew, R., Birt, A., Borger, A., Boyer, T., Broersma, J. A., Cheng, L., Dentener, F., Friedlingstein, P., Gutiérrez, J. M., Gütschow, J., Hall, B., Ishii, M., Jenkins, S., Lan, X., Lee, J.-Y., Morice, C., Kadow, C., Kennedy, J., Killick, R., Minx, J. C., Naik, V., Peters, G. P., Pirani, A., Pongratz, J., Schleussner, C.-F., Szopa, S., Thorne, P., Rohde, R., Rojas Corradi, M., Schumacher, D., Vose, R., Zickfeld, K., Masson-Delmotte, V., and Zhai, P.: Indicators of Global Climate Change 2022: annual update of large-scale indicators of the state of the climate system and human influence, Earth Syst. Sci. Data, 15, 2295–2327, https://doi.org/10.5194/essd-15-2295-2023, 2023.

Fuglestvedt, J., Berntsen, T., Myhre, G., Rypdal, K., and Skeie, R. B.: Climate forcing from the transport sectors, P. Natl. Acad. Sci. USA, 105, 454–458, https://doi.org/10.1073/pnas.0702958104, 2008.

Gettelman, A., Christensen, M. W., Diamond, M. S., Gryspeerdt, E., Manshausen, P., Stier, P., Watson-Parris, D., Yang, M., Yoshioka, M., and Yuan, T.: Has Reducing Ship Emissions Brought Forward Global Warming?, Geophys. Res. Lett., 51, e2024GL109077, https://doi.org/10.1029/2024GL109077, 2024.

Glassmeier, F., Hoffmann, F., Johnson, J. S., Yamaguchi, T., Carslaw, K. S., and Feingold, G.: Aerosol–cloud-climate cooling overestimated by ship-track data, Science, 371, 485–489, https://doi.org/10.1126/science.abd3980, 2021.

Hansen, J. E., Sato, M., Simons, L., Nazarenko, L. S., Sangha, I., Kharecha, P., Zachos, J. C., von Schuckmann, K., Loeb, N. G., Osman, M. B., Jin, Q., Tselioudis, G., Jeong, E., Lacis, A., Ruedy, R., Russell, G., Cao, J., and Li, J.: Global warming in the pipeline, Oxford Open Climate Change, 3, kgad008, https://doi.org/10.1093/oxfclm/kgad008, 2023.

Hoesly, R. and Smith, S.: CEDS v_2024_04_01 Release Emission Data, Version v_2024_04_01, Zenodo [data set], https://doi.org/10.5281/zenodo.10904361, 2024.

IMO: Amendments to the Annex of the Protocol of 1997 to amend the International Convention for the Prevention of Pollution from Ships, 1973, as modified by the Protocol of 1978 relating thereto, Amendments to MARPOL Annex VI, RESOLUTION MEPC.305(73), https://wwwcdn.imo.org/localresources/en/OurWork/Environment/Documents/Air%20pollution/MEPC.305%2873%29.pdf (last access: 23 April 2024), 2018.

Jin, Q., Grandey, B. S., Rothenberg, D., Avramov, A., and Wang, C.: Impacts on cloud radiative effects induced by coexisting aerosols converted from international shipping and maritime DMS emissions, Atmos. Chem. Phys., 18, 16793–16808, https://doi.org/10.5194/acp-18-16793-2018, 2018.

Kelley, M., Schmidt, G. A., Nazarenko, L. S., Bauer, S. E., Ruedy, R., Russell, G. L., Ackerman, A. S., Aleinov, I., Bauer, M., Bleck, R., Canuto, V., Cesana, G., Cheng, Y., Clune, T. L., Cook, B. I., Cruz, C. A., Del Genio, A. D., Elsaesser, G. S., Faluvegi, G., Kiang, N. Y., Kim, D., Lacis, A. A., Leboissetier, A., LeGrande, A. N., Lo, K. K., Marshall, J., Matthews, E. E., McDermid, S., Mezuman, K., Miller, R. L., Murray, L. T., Oinas, V., Orbe, C., García-Pando, C. P., Perlwitz, J. P., Puma, M. J., Rind, D., Romanou, A., Shindell, D. T., Sun, S., Tausnev, N., Tsigaridis, K., Tselioudis, G., Weng, E., Wu, J., and Yao, M.-S.: GISS-E2.1: Configurations and Climatology, J. Adv. Model. Earth Sy., 12, e2019MS002025, https://doi.org/10.1029/2019MS002025, 2020.

Kirkevåg, A., Iversen, T., Seland, Ø., Hoose, C., Kristjánsson, J. E., Struthers, H., Ekman, A. M. L., Ghan, S., Griesfeller, J., Nilsson, E. D., and Schulz, M.: Aerosol–climate interactions in the Norwegian Earth System Model – NorESM1-M, Geosci. Model Dev., 6, 207–244, https://doi.org/10.5194/gmd-6-207-2013, 2013.

Kirkevåg, A., Grini, A., Olivié, D., Seland, Ø., Alterskjær, K., Hummel, M., Karset, I. H. H., Lewinschal, A., Liu, X., Makkonen, R., Bethke, I., Griesfeller, J., Schulz, M., and Iversen, T.: A production-tagged aerosol module for Earth system models, OsloAero5.3 – extensions and updates for CAM5.3-Oslo, Geosci. Model Dev., 11, 3945–3982, https://doi.org/10.5194/gmd-11-3945-2018, 2018.

Lauer, A., Eyring, V., Hendricks, J., Jöckel, P., and Lohmann, U.: Global model simulations of the impact of ocean-going ships on aerosols, clouds, and the radiation budget, Atmos. Chem. Phys., 7, 5061–5079, https://doi.org/10.5194/acp-7-5061-2007, 2007.

Liu, X., Ma, P.-L., Wang, H., Tilmes, S., Singh, B., Easter, R. C., Ghan, S. J., and Rasch, P. J.: Description and evaluation of a new four-mode version of the Modal Aerosol Module (MAM4) within version 5.3 of the Community Atmosphere Model, Geosci. Model Dev., 9, 505–522, https://doi.org/10.5194/gmd-9-505-2016, 2016.

Lund, M. T., Myhre, G., Haslerud, A. S., Skeie, R. B., Griesfeller, J., Platt, S. M., Kumar, R., Myhre, C. L., and Schulz, M.: Concentrations and radiative forcing of anthropogenic aerosols from 1750 to 2014 simulated with the Oslo CTM3 and CEDS emission inventory, Geosci. Model Dev., 11, 4909–4931, https://doi.org/10.5194/gmd-11-4909-2018, 2018.

Manshausen, P., Watson-Parris, D., Christensen, M. W., Jalkanen, J.-P., and Stier, P.: Invisible ship tracks show large cloud sensitivity to aerosol, Nature, 610, 101–106, https://doi.org/10.1038/s41586-022-05122-0, 2022.

Manshausen, P., Watson-Parris, D., Christensen, M. W., Jalkanen, J.-P., and Stier, P.: Rapid saturation of cloud water adjustments to shipping emissions, Atmos. Chem. Phys., 23, 12545–12555, https://doi.org/10.5194/acp-23-12545-2023, 2023.

McDuffie, E. E., Smith, S. J., O'Rourke, P., Tibrewal, K., Venkataraman, C., Marais, E. A., Zheng, B., Crippa, M., Brauer, M., and Martin, R. V.: A global anthropogenic emission inventory of atmospheric pollutants from sector- and fuel-specific sources (1970–2017): an application of the Community Emissions Data System (CEDS), Earth Syst. Sci. Data, 12, 3413–3442, https://doi.org/10.5194/essd-12-3413-2020, 2020.

Menon, S. and Rotstayn, L.: The radiative influence of aerosol effects on liquid-phase cumulus and stratiform clouds based on sensitivity studies with two climate models, Clim. Dynam., 27, 345–356, https://doi.org/10.1007/s00382-006-0139-3, 2006.

Myhre, G., Aas, W., Cherian, R., Collins, W., Faluvegi, G., Flanner, M., Forster, P., Hodnebrog, Ø., Klimont, Z., Lund, M. T., Mülmenstädt, J., Lund Myhre, C., Olivié, D., Prather, M., Quaas, J., Samset, B. H., Schnell, J. L., Schulz, M., Shindell, D., Skeie, R. B., Takemura, T., and Tsyro, S.: Multi-model simulations of aerosol and ozone radiative forcing due to anthropogenic emission changes during the period 1990–2015, Atmos. Chem. Phys., 17, 2709–2720, https://doi.org/10.5194/acp-17-2709-2017, 2017.

O'Rourke, P. R., Smith, S. J., Mott, A., Ahsan, H., McDuffie, E. E., Crippa, M., Klimont, Z., McDonald, B., Wang, S., Nicholson, M. B., Feng, L., and Hoesly, R. M.: CEDS v_2021_04_21 Release Emission Data (v_2021_02_05), Zenodo [data set], https://doi.org/10.5281/zenodo.4741285, 2021.

Partanen, A. I., Laakso, A., Schmidt, A., Kokkola, H., Kuokkanen, T., Pietikäinen, J.-P., Kerminen, V.-M., Lehtinen, K. E. J., Laakso, L., and Korhonen, H.: Climate and air quality trade-offs in altering ship fuel sulfur content, Atmos. Chem. Phys., 13, 12059–12071, https://doi.org/10.5194/acp-13-12059-2013, 2013.

Santos, L. F. E. D., Salo, K., Kong, X., Hartmann, M., Sjöblom, J., and Thomson, E. S.: Marine Fuel Regulations and Engine Emissions: Impacts on Physicochemical Properties, Cloud Activity and Emission Factors, J. Geophys. Res., 129, e2023JD040389, https://doi.org/10.1029/2023JD040389, 2024.

Seland, Ø., Bentsen, M., Olivié, D., Toniazzo, T., Gjermundsen, A., Graff, L. S., Debernard, J. B., Gupta, A. K., He, Y.-C., Kirkevåg, A., Schwinger, J., Tjiputra, J., Aas, K. S., Bethke, I., Fan, Y., Griesfeller, J., Grini, A., Guo, C., Ilicak, M., Karset, I. H. H., Landgren, O., Liakka, J., Moseid, K. O., Nummelin, A., Spensberger, C., Tang, H., Zhang, Z., Heinze, C., Iversen, T., and Schulz, M.: Overview of the Norwegian Earth System Model (NorESM2) and key climate response of CMIP6 DECK, historical, and scenario simulations, Geosci. Model Dev., 13, 6165–6200, https://doi.org/10.5194/gmd-13-6165-2020, 2020.

Sherwood, S. C., Bony, S., Boucher, O., Bretherton, C., Forster, P. M., Gregory, J. M., and Stevens, B.: Adjustments in the Forcing-Feedback Framework for Understanding Climate Change, B. Am. Meteorol. Soc., 96, 217–228, https://doi.org/10.1175/BAMS-D-13-00167.1, 2015.

Skeie, R. B.: ragnhibs/imo2020: V1.1, Zenodo [data set/code], https://doi.org/10.5281/zenodo.13710977, 2024.

Skeie, R. B., Hodnebrog, Ø., and Myhre, G.: Trends in atmospheric methane concentrations since 1990 were driven and modified by anthropogenic emissions, Communications Earth & Environment, 4, 317, https://doi.org/10.1038/s43247-023-00969-1, 2023.

Skeie, R. B., Hodnebrog, Ø., Jouan, C., and Byrom, R.: Multi-model results of 2020 shipping regulation, Norstore [data set], https://doi.org/10.11582/2024.00157, 2024.

Smith, C. J., Kramer, R. J., Myhre, G., Forster, P. M., Soden, B. J., Andrews, T., Boucher, O., Faluvegi, G., Fläschner, D., Hodnebrog, Ø., Kasoar, M., Kharin, V., Kirkevåg, A., Lamarque, J. F., Mülmenstädt, J., Olivié, D., Richardson, T., Samset, B. H., Shindell, D., Stier, P., Takemura, T., Voulgarakis, A., and Watson-Parris, D.: Understanding Rapid Adjustments to Diverse Forcing Agents, Geophys. Res. Lett., 45, 12023–12031, https://doi.org/10.1029/2018GL079826, 2018.

Smith, C. J., Kramer, R. J., Myhre, G., Alterskjær, K., Collins, W., Sima, A., Boucher, O., Dufresne, J.-L., Nabat, P., Michou, M., Yukimoto, S., Cole, J., Paynter, D., Shiogama, H., O'Connor, F. M., Robertson, E., Wiltshire, A., Andrews, T., Hannay, C., Miller, R., Nazarenko, L., Kirkevåg, A., Olivié, D., Fiedler, S., Lewinschal, A., Mackallah, C., Dix, M., Pincus, R., and Forster, P. M.: Effective radiative forcing and adjustments in CMIP6 models, Atmos. Chem. Phys., 20, 9591–9618, https://doi.org/10.5194/acp-20-9591-2020, 2020.

Sofiev, M., Winebrake, J. J., Johansson, L., Carr, E. W., Prank, M., Soares, J., Vira, J., Kouznetsov, R., Jalkanen, J.-P., and Corbett, J. J.: Cleaner fuels for ships provide public health benefits with climate tradeoffs, Nat. Commun., 9, 406, https://doi.org/10.1038/s41467-017-02774-9, 2018.

Stjern, C. W., Forster, P. M., Jia, H., Jouan, C., Kasoar, M. R., Myhre, G., Olivié, D., Quaas, J., Samset, B. H., Sand, M., Takemura, T., Voulgarakis, A., and Wells, C. D.: The Time Scales of Climate Responses to Carbon Dioxide and Aerosols, J. Climate, 36, 3537–3551, https://doi.org/10.1175/JCLI-D-22-0513.1, 2023.

Szopa, S., Naik, V., Adhikary, B., Artaxo, P., Berntsen, T., Collins, W. D., Fuzzi, S., Gallardo, L., Kiendler Scharr, A., Klimont, Z., Liao, H., Unger, N., and Zanis, P.: Short-Lived Climate Forcers, in: Climate Change 2021: The Physical Science Basis. Contribution of Working Group I to the Sixth Assessment Report of the Intergovernmental Panel on Climate Change, edited by: Masson-Delmotte, V., Zhai, P., Pirani, A., Connors, S. L., Péan, C., Berger, S., Caud, N., Chen, Y., Goldfarb, L., Gomis, M. I., Huang, M., Leitzell, K., Lonnoy, E., Matthews, J. B. R., Maycock, T. K., Waterfield, T., Yelekçi, O., Yu, R., and Zhou, B., Cambridge University Press, Cambridge, United Kingdom and New York, NY, USA, https://doi.org/10.1017/9781009157896.008, 2021.

Søvde, O. A., Prather, M. J., Isaksen, I. S. A., Berntsen, T. K., Stordal, F., Zhu, X., Holmes, C. D., and Hsu, J.: The chemical transport model Oslo CTM3, Geosci. Model Dev., 5, 1441–1469, https://doi.org/10.5194/gmd-5-1441-2012, 2012.

Watson-Parris, D., Christensen, M. W., Laurenson, A., Clewley, D., Gryspeerdt, E., and Stier, P.: Shipping regulations lead to large reduction in cloud perturbations, P. Natl. Acad. Sci. USA, 119, e2206885119, https://doi.org/10.1073/pnas.2206885119, 2022.

Yuan, T., Song, H., Wood, R., Wang, C., Oreopoulos, L., Platnick, S. E., von Hippel, S., Meyer, K., Light, S., and Wilcox, E.: Global reduction in ship-tracks from sulfur regulations for shipping fuel, Science Advances, 8, eabn7988, https://doi.org/10.1126/sciadv.abn7988, 2022.

Yuan, T., Song, H., Oreopoulos, L., Wood, R., Bian, H., Breen, K., Chin, M., Yu, H., Barahona, D., Meyer, K., and Platnick, S.: Abrupt reduction in shipping emission as an inadvertent geoengineering termination shock produces substantial radiative warming, Communications Earth & Environment, 5, 281, https://doi.org/10.1038/s43247-024-01442-3, 2024.